Significance and Mapping of the Sea Surface Temperature (SST) With the Aid of the Earth Engine Cloud Computing Approach

Newman Enyioko (PhD)
Medonice Consulting and Research Institute
newmanenyioko@yahoo.com

Abstract

The study examined the significance and mapping of the sea surface temperature (SST) with the aid of the earth engine cloud computing approach. Mapping of the sea surface temperature is important for fisheries industry to increase the opportunity to catch the fish. Traditional methods to monitor this phenomenon is by using the remote sensing techniques. However, conventional remote sensing methods is need higher computer specifications as well as larger space of hard disk drive and commercial software to process the datasets. The availability of the earth engine cloud-computing approach provides benefit for researcher to increase the efficiency and effectivity of large-scale imageries processing. The study revealed that the sea surface temperature (SST) is very significant as it is a key variable in both oceanographic and atmospheric studies. It is the lower boundary condition for atmospheric numerical models, essential in their ability to support accurate forecasts. The sea surface temperature (SST) is a critical parameter for weather and climate research as well as oceanography. Critically, as revealed by the study, sea surface temperature (SST) is one of the oldest and best documented Essential Climate Variables (ECV). The global SST distribution is directly related to the sources and sinks of heat at the surface. The factors which contribute to an increase in SST are incoming shortwave radiation from the Sun, incoming longwave radiation from the atmosphere, conduction of warmer air toward cooler water, gain of latent heat through condensation and movement (advection) of warmer water into the region. This study proposedthe sate-of-the-art cloud-computing platform of GEE to monitor and map the sea surface temperature and total suspended matter for long periods of analysis of Timor Sea, Van DiemenGulf, and Beagle Gulf/. In total there more than 600 of global images Collection 1 Tier 1 calibrated top-of-atmosphere (TOA) reflectance is used and obtained within the GEE platform. The Radiative transfer equation (RTE) method is used to extract the surface temperature. To extract the total suspended matter, the Sentinel-3 Ocean and Land Color Instrument Earth Observation Full Resolution (OLCI EFR) is used. The Case-2 Regional CoastColour (C2RCC) processor within the SentiNel Application Platform (SNAP) software isused. The study revealed that the GEE platform is successfully captured the dynamic sea surface temperature as well as the total suspended matter with high efficiency in term of time and hard disk drive consumption.

Keywords: Sea Surface Temperature, Sea Mapping, Earth Engine, Cloud Computing, Global Images, Visualization Parameters

Introduction

The sea surface temperature of global open ocean has been increased around 0.11°C per decade on average, while the coastal areas have been increased around 0.18±0.16°C per decade on average (Mardani et al. 2019). This situation is likely to cause the fluctuations of the fisheries production. The tropical regions will face decrease up to 40%, while the high latitude regions could increase the marine capture fisheries around 30%to 70% (Deines et al. 2019).

One of many variables that influence the fisheries productions is sea surface temperatures. Some researchers have been tried to utilized the medium and higher spatial resolution to produce sea surface temperature such as MERIS and Landsat images. For instance, research by Uiboupin et al (2016] monitor the upwelling events in the Gulf of Finland using MERIS images. They compared the surface temperature with the chlorophyll *a* (Chl *a*) distributionand found the consistent relation between those parameters. Meanwhile, Aleskerova et al [3] retrieved sea surface temperature of Black Sea using The earth engine cloud computing and two-channel method. They found that the result of The earth engine cloud computing andMODIS images only have small differences in surface temperature mapping, it is around 0.58°C (Vanhellemont, 2021).

However, the previous studies have also shown that the procedure to retrieved sea surface temperature is need large size of satellite image, high computer specification, and utilization of commercial software. This traditionalmethod is considered as time-consuming and costly method. The objective of this study is to propose new method based-on cloud-computing geocomputation platform of Google Earth Engine (GEE) to retrieve sea surface temperature information from thermal channel of The earth engine cloud computing (Deines et al. 2019).

GEE is cloud-computing platform to process large scale satellite images that available free for public (Deines et al. 2019). Overtwenty petabyte of satellite imagery and geospatial datasets is available for everyone to analyses and monitor theearth's surface. To operate the GEE platform, we need to work based on code editor using JavaScript. The GEE platform could be accessed through http://code.earthengine.google.com/

Some researchers have been used the GEE platform to analyses the land cover mapping,, annual irrigation, wetland inventory, mapping particulate matter, mapping shorelines, and mapping wetland (Mardani et al. 2019).. However, based on our current knowledge, there is very limited research using GEE to monitor the sea surface temperature and total suspended matter.

The Concept of Sea Surface Temperature (SST)

Sea surface temperature (SST) is a challenging parameter to define precisely as the upper ocean (~10 m) has a complex and variable vertical temperature structure that is related to ocean turbulence and air-sea fluxes of heat, moisture and momentum (Deines et al. 2019). A theoretical framework is therefore required to understand the information content and relationships between measurements of SST made by different satellite and in situ instruments, especially if these are to be merged together. The definitions of SST developed by the GHRSST

Science Team achieve the closest possible coincidence between what is defined and what can be measured, considering current scientific knowledge and understanding of the near surface thermal structure of the ocean (Vanhellemont, 2021).

The concept of sea surface temperature (SST) in the upper 10 m of the ocean and provides a framework to understand the differences between complementary sea surface temperature (SST) measurements. It encapsulates the effects of dominant heat transport processes and time scales of variability associated with distinct vertical and volume regimes of the upper ocean water column (horizontal and temporal variability is implicitly assumed (Mardani et al. 2019).

The Significance of Mapping the sea surface temperature (SST)

The sea surface temperature (SST) is a key variable in both oceanographic and atmospheric studies. It is the lower boundary condition for atmospheric numerical models, essential in their ability to support accurate forecasts. For example, warm ocean temperatures feed hurricanes, and thus accurate knowledge of SST (and the heat potential under the surface) helps forecast their path and intensity (Deines et al. 2019). Ocean temperatures, as reflected in SST, influence fish feeding and reproductive behaviour. Temperature 'fronts', where there is a strong gradient in temperature (often extending several tens of metres vertically), encourage the growth of plankton and thus attract fish to feed on the plankton, or on other fish; at such fronts, fish display reproductive behaviour such as changing vertical position and forming schools. Ocean temperatures affect corals, and SST is used to evaluate coral bleaching. Eddies are the storms of the sea carrying trapped ocean properties, and they can be recognized in sea surface temperature (SST) as well as in sea surface height. SST is a central factor in studies of air sea fluxes, and as an indicator for inter-annual variability as well as climate variation. The onset of the well-known El Niño / La Niña cycles can be easily recognized in sea surface temperature (SST) (Vanhellemont, 2021)

The sea surface temperature (SST) is a critical parameter for weather and climate research as well as oceanography. Indeed, sea surface temperature (SST) is one of the oldest and best documented Essential Climate Variables (ECV). The global SST distribution is directly related to the sources and sinks of heat at the surface. The factors which contribute to an increase in SST are incoming shortwave radiation from the Sun, incoming longwave radiation from the atmosphere, conduction of warmer air toward cooler water, gain of latent heat through condensation and movement (advection) of warmer water into the region. The factors which contribute to a decrease in SST are the emission of longwave radiation from the surface to the atmosphere, conduction of warmer water toward cooler air, loss of latent heat through evaporation and movement (advection) of cooler water into the region. Naturally, the sea surface temperature (SST) will increase if the net effect of these processes is such that the ocean surface receives more energy than it loses (Deines et al. 2019).

1. Time Series of Global Images

In the time series features are extracted from images using image processing techniques. We

considertwo different image feature extraction approaches: spatial bag-of-features (SBoF) model and convolutional neural networks (CNNs). We describe the details in the following sections.

The study use recurrence plots (RPs) to encode time series data into images, which provides a way to visualize the periodic nature of a trajectory through a phase space and can contain all relevant dynamical information in the time series (Mardani et al. 2019). A recurrence plot of time series *x*, showing when the time series revisits a previous state, can be formulated as $\boldsymbol{R(i,j) = \Theta(\epsilon - |x_i - x_j|)}$.

Where $R(i, j)$ is the element of the recurrence matrix R, i indexes time on the x-axis of the recurrence plot, and $\boldsymbol{j}$ indexes time on the y-axis. ϵ is a predefined threshold, and $\Theta(\cdot)$ is the Heaviside step function. In short, one draws a black dot when x_i and x_j are closer than ϵ. Instead of binary output, an un-thresholded RP is not binary but difficult to quantify. We usethe following modified RP, which balances the binary output and un-

It gives more values than a binary RP and results in colored plots. Figure 1 shows three typical examples of recurrence plots. They reveal different patterns of recurrence plots for time series with randomness, periodicity, chaos, and trend. We can see that the recurrence plots shown in the right column well depict the pre-defined patterns in the time series shown in the left column (Vanhellemont, 2021).

The original bag-of-features (BoF) model, which extracts features from one-dimensional sig- nal segments, has achieved great success in time series classification (Deines et al. 2019). transformed a time series into two-dimensional recur- rence images with a recurrence plot (Deines et al. 2019) and then applied the BoF model. Extracting time series features is then equivalent to identifying key points in images, whichare called key descriptors. A promising algorithm is the SIFT algorithm, whichis used to detect and describe local features in images by identifying the maxima/minima ofthe difference of Gaussians (DoG) that occur at the multiscale spaces of an image as its key descriptors. It consists of the following four steps (Mardani et al. 2019).

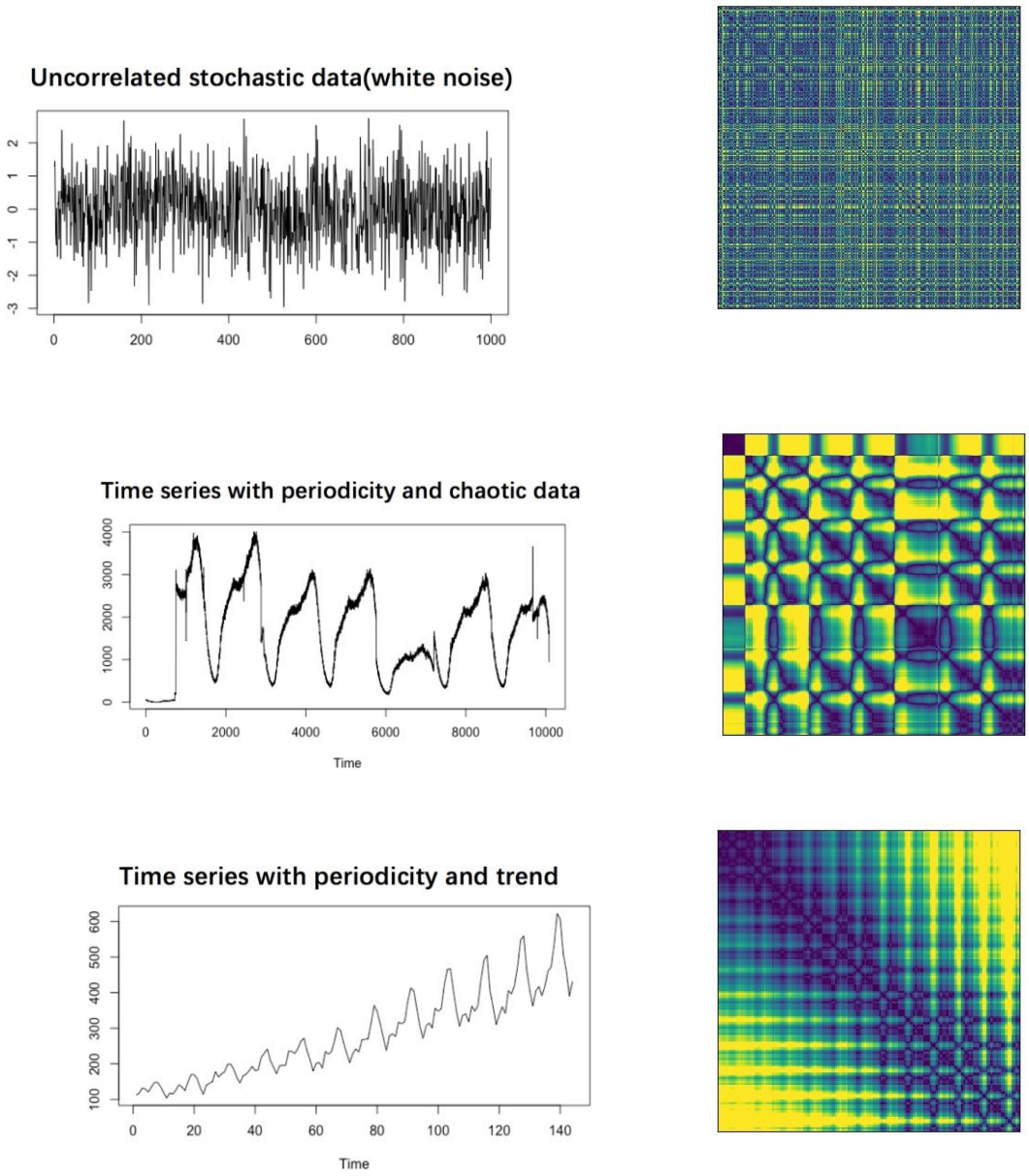

Figure 1. Typical examples of recurrence plots (right column) for time series data with different patterns (left column): uncorrelated stochastic data, i.e., white noise (top), a time series with periodicity and chaos (middle), and a time series with periodicity and trend (bottom).

NASA, (2019). Landsat 7 (L7) Data Users Handbook, **7** (11), 106, https://prd-wret.s3.us-west-2.amazonaws.com/assets/palladium/production/atoms/files/LSDS-1927_L7_Data_Users_Handbook-v2.pdf.

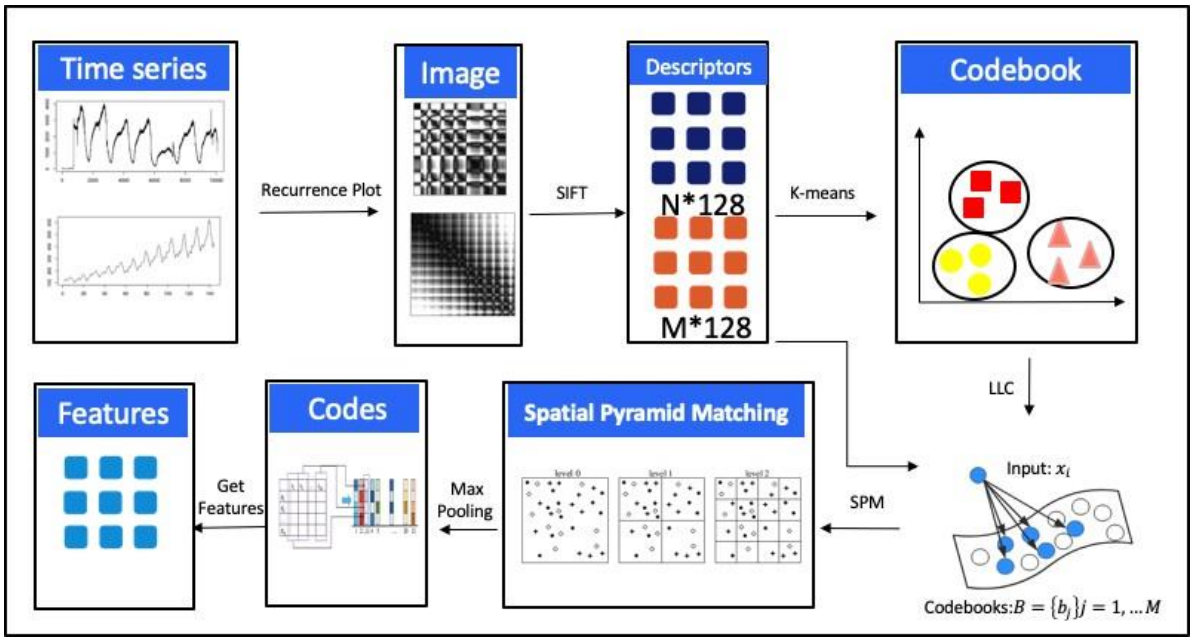

Figure 2. Image-based time series feature extraction with spatial bag-of-features model.

Source: ESA, (2020). OLCI Instrument Payload, *ESA Sentin.* 5, 21-35 https://sentinels.copernicus.eu/web/sentinel/missions/sentinel-3/instrument-payload/olci.

It consists of four steps:

(i) encode a time series as an image with recurrence plots; (ii) detect key points with SIFT and obtain the basic descriptors with *k*-means for the codebook; (iii) generate the representation based on LLC; and (iv) extract spatial information via SPM and max pooling (Deines et al. 2019).

Within the neighborhood around each feature point, the local gradient of the image is measured at selected scales, which is transformed into a repre- sentation that allows larger local shape deformations and illumination transformations. The SIFT method uses a 128-dimensional vector to characterize the key descriptors in an image. First, an 8-direction histogram is established in each 4 × 4 subregion, and 16 subregions around the key points are used. We then calculate the magnitude and directionof each pixel's gradient magnitude and add it to the corresponding subregion. In the end, 128-

dimensional image data based on histograms are generated (Vanhellemont, 2021).

Each descriptor can be projected onto its local coordinate system, and the projected coordinates are integrated by max pooling to generate the final representation with the LLC method, which utilizes the locality constraints to project each descriptor onto its local coordinate system (Deines et al. 2019).

The basic descriptors $B \in R^{128\times M}$ are obtained by *k*-means clustering. The locality adaptor d_i givesdifferent freedom for each basis vector proportional to its similarity to the input descriptor. We use σ to adjust the weight decay speed for the locality adaptor, and λ is the adjustment factor. However, in reality, the number of descriptors obtained by the SIFT algorithm is usually huge.To address this problem, Vanhellemont (2021) proposed an incremental codebook optimization method for LLC.

The bag-of-features model calculates the distribution characteristics of feature points in the whole image and then generates a global histogram. As a result, the image's spatial distribution information is lost, and the image may not be accurately described. To obtain the spatial information of images, we apply a spatial pyramid matching (SPM) method, which statistically distributes image feature points at different resolutions and has achieved high accuracy on a large dataset of 15 natural scene categories (Deines et al. 2019). The image is divided into progressively finer grid sequences at each level of the pyramid, and features are derived fromeach grid and combined into one large feature vector. Fig. 3 depicts the diagram of the SPMand max pooling process. In this task, we divide the image by 1×1, 2×2 and 4×4, and thus obtain 21 subregions. To obtain the representation for each subregion, we first obtain the descriptors. Suppose that we obtain 12 descriptors denoted by $\boldsymbol{D_i} \in \boldsymbol{R}^{12\times 200}$ for the third region (the dimension of the local linear representation of the descriptors is equal to 200). We thencan obtain the maximum value of every dimension of $\boldsymbol{D_i}$. After max pooling, we calculate the feature representation denoted by $\boldsymbol{f_i} \in \boldsymbol{R}^{200\times 1}$ for the third region. The feature representationsof the other twenty regions can be obtained in the same way. Finally, the 21 features are linked together for the final representation of the time series (Mardani et al. 2019).

2. Filter 15 Days in August, 2021

The global mean temperature in 2021 is estimated to have been 1.21 °C (2.17 °F) above the average temperature from 1850-1900, a period often used as a pre-industrial baseline for global temperature targets. This is ~0.15 °C (~0.28 °F) cooler than in 2021.

The sea surface temperature of the study area during the periods of analysis is shown in Figure. 2. We exclude the temperature below 10°C since we assumed it was cloud cover. In total there are more than 125 of 650 images were excluded from the analysis due to very low surface temperature.

The trend of sea surface temperature during period of analysis is very dynamic. We found the low sea surface temperature is occurred every March to August each year. While the higher sea surface temperature is occurred every September to November, and it became low again during December to February, however it is still higher than periods of March to August (Deines et al. 2019).

The study by Vanhellemont (2021) found that the year 2015 and 2021 are the hottest year compared to other period of analysis. From January to December of 2015 and 2021, the average sea surface temperature of the study areas is higher than other periods of analysis, in average 22.7°C and 22.4°C respectively. Year 2016 is selected since it shows the lowest average sea surface temperature, 20°C. While August 2021 is selected due to that month show clear cloud coverage and has the lowest average temperature of 18.3°C.

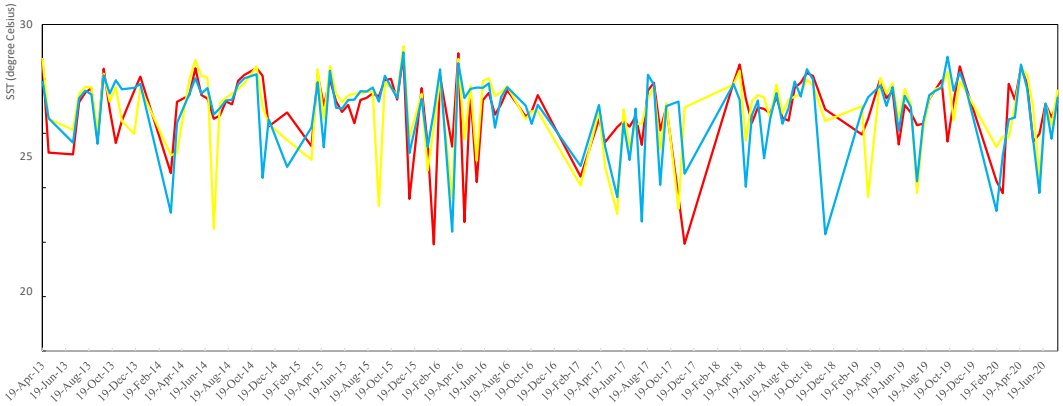

Figure 3: The surface temperature (SST) of three study areas from 2013 to 2021. Time series

NASA, (2019). Landsat 7 (L7) Data Users Handbook, **7** (11), 106, https://prd-wret.s3.us-west-2.amazonaws.com/assets/palladium/production/atoms/files/LSDS-1927_L7_Data_Users_Handbook-v2.pdf.

After we validated the low sea surface temperature of August 2021 with the Sentinel-3 OLCI EFR datasets we found positive result. The result of Sentinel-3 OLCI EFR found

high concentration of total suspended matter. during the low sea surface temperature event. Therefore, we could conclude that even in low sea surface temperature the suspended matter is still can be found (Vanhellemont, 2021).

The result of this study is consistent with the research by Mardani et al.(2019), who used different satellite sensor and remote sensing technique of the same study area. The total suspended matter is relatively high in dry season due to tidal-driven resuspension amplified by wind and low in wet season due toriver run-off into the Van Diemen Gulf is filtered by the wetland of Kakadu National Park. The study found that the maximum total suspended matter in August 2021 was ranging between 200-300 g m-3,while the minimum average values ranging between 50-100 g m-3.

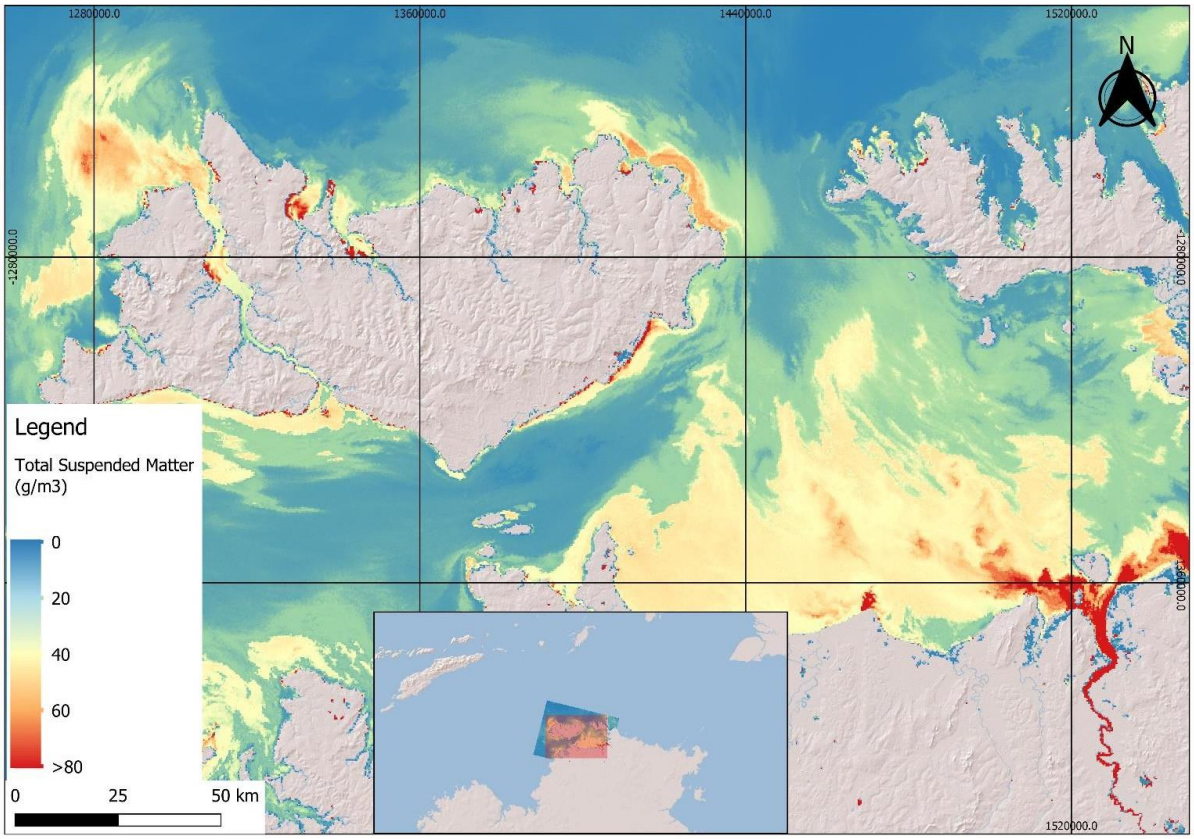

Figure 4: The map of total suspended matter (TSM) of the study areas.

Source: ESA, (2020). OLCI Instrument Payload, *ESA Sentin.* 5, 21-35 https://sentinels.copernicus.eu/web/sentinel/missions/sentinel-3/instrument-payload/olci.

3.Water Temperature at 0 Meter Scaled to Degree Celsius

The study found that the result of The earth engine cloud computing andMODIS images only have small differences in surface temperature mapping, it is around 0.58°C.

However, the previous studies have also shown that the procedure to retrieved sea surface temperature is need large size of satellite image, high computer specification, and utilization of commercial software. This traditional method is considered as time-consuming and costly method. The objective of this study is to propose new method based-on cloud-computing geo computation platform of Google Earth Engine (GEE) to retrieve sea surface temperature information from thermal channel of The earth engine cloud computing. GEE is cloud-computing platform to process large scale satellite images that available free for public (Mardani et al. 2019). Over twenty petabyte of satellite imagery and geospatial datasets is available for everyone to analyses and monitor the earth's surface. To operate the GEE platform, we need to work based on code editor using JavaScript. The GEE platform could be accessed through http://code.earthengine.google.com/

Some researchers have been used the GEE platform to analyses the land cover mapping [5], annual irrigation, wetland inventory, mapping particulate matter, mapping shorelines and mapping wetland (Deines et al. 2019). However, based on our current knowledge, there is very limited research using GEE to monitor the sea surface temperature and total suspended matter.

Therefore, this study provides the first detailed record of total suspended matter and the sea surface temperature information around Timor Sea, Van Diemen Gulf, and Beagle Gulf. Seven years of The earth engine cloud computing observation, from 2013-2021 is used with special focus in the August 2021 (Vanhellemont, 2021).

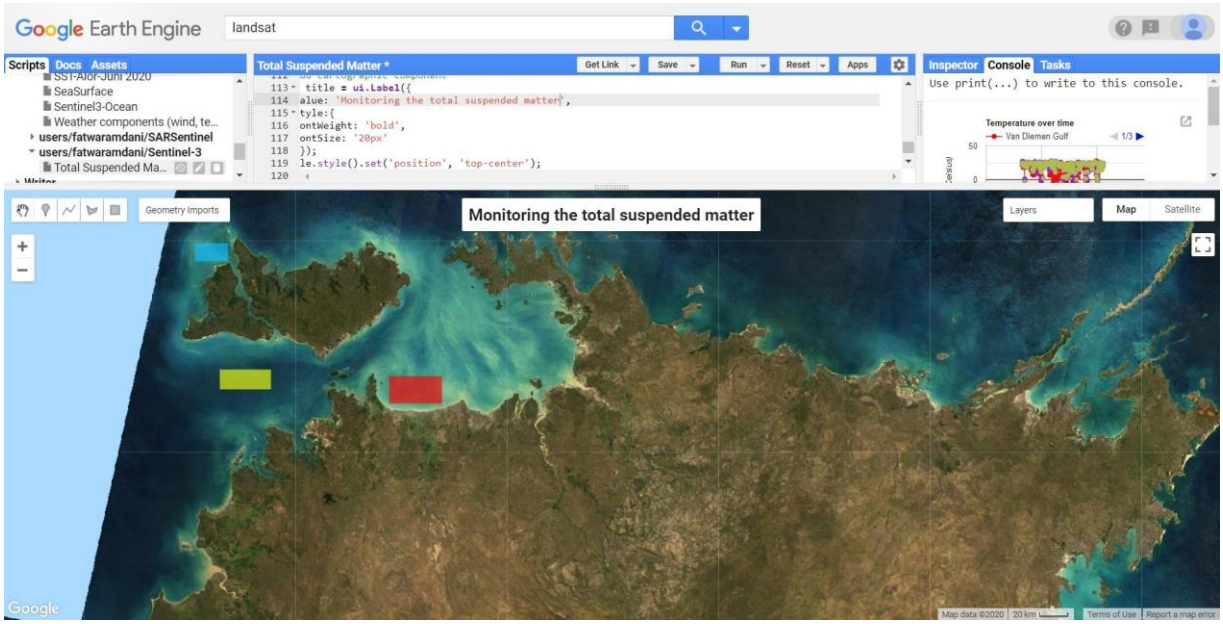

Figure 5. Study area as shown within the GEE platform

Source: Developer, G. (2020). Sentinel-3 OLCI EFR: Ocean and Land Color Instrument Earth Observation Full Resolution, *Earth Engine Data Cat, 5, 34-48.* https://developers.google.com/earth-ngine/datasets/catalog/COPERNICUS_S3_OLCI#description.

Radiative transfer equation (RTE) method is chooses based on the research by reference (Deines et al. 2019). They research found that when using Landsat 8 Thermal Infrared Sensor (TIRS) data, RTE method produced the best results compared to Mono Window Algorithm (MWA) and Single-Channel Algorithm (SCA). RTE method is a straightforward technique to produce surface temperature from a single TIR band. In this studywe used band 10 of Landsat 8 to retrieve sea surface temperature. Since based on the research by Deines et al. (2019) band 10 has lower Root Mean Squared Difference (RMSD) of 0.7 Kelvin, compared to band 11 with 1 Kelvin RMSD.To produce the sea surface temperature from band 10 we need to convert the digital number(s) into radiance and then convert the radiance into top of atmosphere brightness temperature. The equation to convert digital number(s) into radiance is as shown in equation (Mardani et al. 2019).

$L_\lambda = M_L * Q_{cal} + A_L L_\lambda = M_L * Q_{cal} + A_L$ (1)

Where:

$L_\lambda L_\lambda$

$M_L M_L$ = Radiance multiplicative scaling factor for the band (RADIANCE_MULT_BAND_10 from the metadata)

Lג Lג= Spectral radiance (W/(m2*srad*µm)

$A_L A_L$ = Radiance additive scaling factor for the band (RADIANCE_ADD_BAND_10 from themetadata)

$Q_{cal} Q_{cal}$ = Level-1 pixel value in digital number (DN)

To convert the spectral radiance into top of atmosphere brightness temperature, the equation formula is shown inequation (2)[19]

$$T = \frac{K_2}{ln\left(\frac{K_1}{L_\lambda}+1\right)} T = \frac{K_2}{ln\left(\frac{K_1}{L_\lambda}+1\right)} \quad (2)$$

Where:

= Top of atmosphere brightness temperature (Kelvin)

= Spectral radiance (W/(m2*srad*µm)

= Band 10 of L8 constants (774.89)

= Band 10 of L8 constants (1321.08)

Finally, to convert the top of atmosphere brightness temperature into degree Celsius, the equation (3) formula isused

$$Celsius = K - Celsius = K - \quad (3)$$

Where:

K = Temperature in Kelvin

L_λ *Celsius* = Temperature in Celsius

4. Visualization Parameters

Visualization parameters are graphs, diagrams, charts, and other visual representations such as heat maps used to provide a means of understanding trends, outliers, anomalies, and patterns in data. Data visualization provides a means of understanding the movement of data trends by showing where defined classified groups of data are moving by using different graphical shapes, colors, and sizes.

Visualization parameter provides a degree of technology in this space in the shape of the Analytics Cloud service. This business intelligence technology can generate reports and offers an import/export feature for your spreadsheets and visuals. But this is not necessarily core cloud computing territory. For that reason, we find that earth engine cloud computing platform is keen to integrate openly with many of the usual suspects in this space who have developed more dedicated data visualization solutions (Deines et al. 2019).

When used effectively, good data visualization can offer organizations a representation of real-world business actions, transactions, and processes in graphical form.

But even when using the dedicated software tools in this space, there are limits to functionality. What data visualization doesn't do is provide a means of controlling business actions from the graphical representations themselves. It's not a steering/driving business dashboard in that sense (Deines et al. 2019).

What users can do inside any given data visualization is to ask deeper questions of the datasets presented. If you asked for a visualization of sales by region and then by year, you would typically have the option of going into more granular detail and getting sales by region and then by month, and so on.

5. Display of Mean 15-Day Sea Surface Temperature on the Map.

The SST data presented here are monthly mean values for August (1982-2021). August mean SSTs provide the most appropriate representation of Arctic Ocean summer SSTs because they are not affected by the cooling and subsequent sea-ice growth that typically takes place in the latter half of September. August 2021 mean SSTs ranged from 6° to 10°C in the southeast Chukchi and Barents Seas to around 0° to 3°C in the East Siberian, Kara and Laptev Seas, Baffin Bay and in the ice-free waters east of Greenland (Fig. 1a). August 2021 mean SSTs were notably warm (around 1°-3.5°C warmer than the 1982-2010 August mean) in the Kara and Laptev Seas (Fig. 1b). This is consistent with early-season sea-ice retreat in these regions, and anomalously warm spring 2021 air temperatures over northern Eurasia (see essays Sea Ice and Surface Air Temperature). SSTs in the waters east of Greenland were also warmer (by around NOAA Arctic Report Card 2021 42 1°-3°C) than the 1982-2010 August mean. It is notable that in the same region, summer 2021 surface air temperatures were about 2°-5°C warmer than the 1981-2010 mean (see essay Surface Air Temperature) (Mardani et al. 2019).

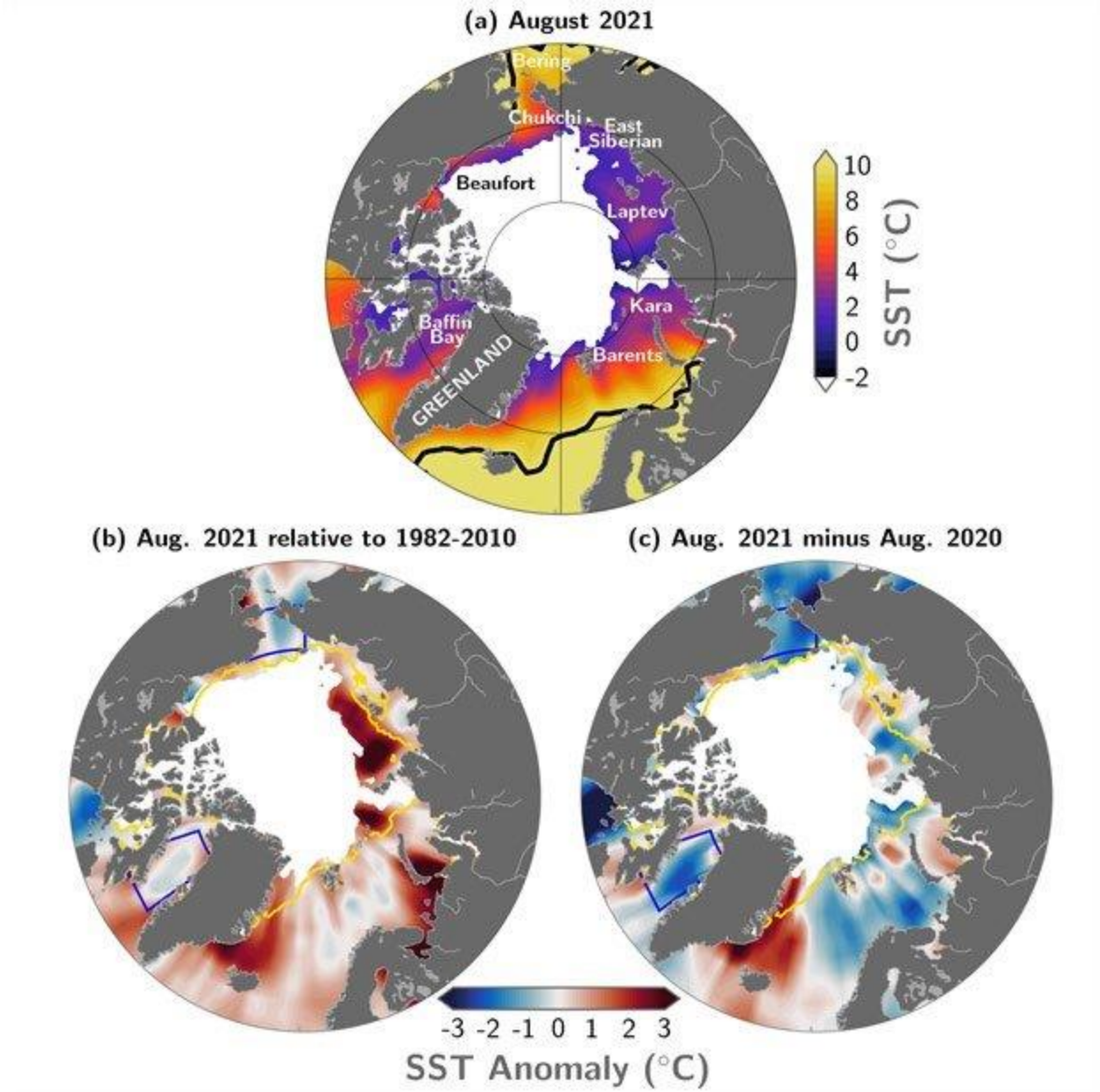

Figure 6: Display of Mean 15-Day Sea Surface Temperature on the Map

Source: Developer, G. (2020). Sentinel-3 OLCI EFR: Ocean and Land Color Instrument Earth Observation FullResolution, *Earth Engine Data Cat, 5, 34-48.* https://developers.google.com/earth-ngine/datasets/catalog/COPERNICUS_S3_OLCI#description.

Figure 64 (a) Mean sea surface temperature (SST; °C) in August 2021. Black contours indicate the 10°C SST isotherm, (b) SST anomalies (°C) in August 2021 relative to the August 1982-2021 mean, (c) Difference between August 2021 SSTs and August 2020 SSTs

(negative values indicate where 2021 was cooler). White shading in all panels is the August 2021 mean sea-ice extent. The yellow lines in (b) and (c) indicate the median ice edge for August 1982-2021. The two regions marked by blue boxes in panels (b) and (c) indicate regions of Baffin Bay and the Chukchi Sea, and relate to data presented in Fig. 2b,c. (Mardani et al. 2019).

It is noticed that many use degrees Fahrenheit, but scientists use Celsius or Kelvin. The study calculated the mean temperature for the first 15 days in August thus:

August date	**High temperature (Degrees F)**
1	3.4
2	3.8
3	4.2
4	4.7
5	5.1
6	5.6
7	6
8	6.5
9	7
10	7.5
11	8
12	8.6
13	9.1
14	9.6
15	10.1

Source: Mardani, M. Mardani, H. De Simone, L. Varas, S., Kita, N. & Saito, T. (2019). Integration of machine learning and open access geospatial data for land cover mapping, *Remote Sens.*, 11 (16**),** 1–17,, doi: 10.3390/rs11161907.

To compute this, the study just needed to add up all of the temperatures and divide by the total number of temperatures (which is 15).

It looks like all of those temperatures added together is 99.2. Now, to find the mean, take 99.2 divided by however many temperatures there were, which was 15. So. 99.2/15 = 6.6. So, the mean is 6.6 degrees F or Celsius (Mardani et al. 2019).

To find the mean you add up all of the values and divide by however many values are present. In our case, we added up the first 15 high temperatures for August, and then divided

by 15. When you are studying climate, it is useful to look at mean temperatures over a long period of time. This allows scientists to see if there is an overall trend in temperature change or if one or two years were just an anomaly (Mardani et al. 2019).

Conclusion

This study evaluated the significance and mapping of the sea surface temperature (SST) with the aid of the earth engine cloud computing approach. Cloud-computing platform ofGEE was used for seven years' periods of analysis. More than 600 images of TIR band of The earth engine cloud computing were acquired. Due to cloud cover, more than 125 images were excluded from the analysis. The excluded images shown very low sea surface temperature, in average below 10°C.

The study revealed that the sea surface temperature (SST) is very significant as it is a key variable in both oceanographic and atmospheric studies. It is the lower boundary condition for atmospheric numerical models, essential in their ability to support accurate forecasts. The sea surface temperature (SST) is a critical parameter for weather and climate research as well as oceanography. Critically, as revealed by the study, sea surface temperature (SST) is one of the oldest and best documented Essential Climate Variables (ECV). The global SST distribution is directly related to the sources and sinks of heat at the surface. The factors which contribute to an increase in SST are incoming shortwave radiation from the Sun, incoming longwave radiation from the atmosphere, conduction of warmer air toward cooler water, gain of latent heat through condensation and movement (advection) of warmer water into the region.

The obtained result showed that the sea surface temperature around the study area is dynamic along the periodsof analysis. The image is clear from cloud coverage and show average sea surface temperature of ~20°C. The periods of low sea surface temperature are found from March to August each year, while the high sea surface temperature is found from September to November each year.

The result indicated that the suspended matter is always transported to the study area in every season along the years. The method used in this study shows very promising since it is very efficient and effective in term of time-consuming as well as the hard disk drive space to save hundreds of files of satellite imageries.

References

Anika, S. & Cassandra, D. Y. (2016). Climate Change Implications for Fisheries and Aquaculture. *Summary of the findings of the IPCC Fifth Assessment Report*, FIAP/C1122.

Aleskerova, A. A. Kubryakov, A. A. & Stanichny, S. V. (2016). A two-channel method for retrieval of the Black Sea surface temperature from The earth engine cloud computing measurements," *Izv. - Atmos. Ocean Phys.*, vol. **52**, no. **9**, pp. 1155–1161, 2016, doi: 10.1134/S0001433816090048.

Deines, J. M. Kendall, A. D., Crowley, M. A., Rapp, J. A. Cardille, J.A. & Hyndman, D. W. (2019). Mapping three decades of annual irrigation across the US High Plains Aquifer using Landsat and Google Earth Engine, *Remote Sens. Environ.*, **233**, . 11,. 11-14 , doi: 10.1016/j.rse.2019.111400.

Developer, G. (2020). Sentinel-3 OLCI EFR: Ocean and Land Color Instrument Earth Observation FullResolution," *Earth Engine Data Cat.*, 2020, [Online]. https://developers.google.com/earth-engine/datasets/catalog/COPERNICUS_S3_OLCI#description.

ESA, (2020). OLCI Instrument Payload, *ESA Sentin.* 5, 21-35 https://sentinels.copernicus.eu/web/sentinel/missions/sentinel-3/instrument-payload/olci.

Gorelick, N. Hancher, M., Dixon, M., Ilyushchenko, D. Thau,S. & Moore, R. (2017). Google Earth Engine:Planetary-scale geospatial analysis for everyone, *Remote Sensing Environment.*, 202, 18–27, doi: 10.1016/j.rse.2017.06.031.

Mardani, M. Mardani, H. De Simone, L. Varas, S., Kita, N. & Saito, T. (2019). Integration of machine learning and open access geospatial data for land cover mapping, *Remote Sens.*, 11 (16**),** 1–17,, doi: 10.3390/rs11161907.

NASA, (2019). Landsat 7 (L7) Data Users Handbook, **7** (11), 106, https://prd-wret.s3.us-west-2.amazonaws.com/assets/palladium/production/atoms/files/LSDS-1927_L7_Data_Users_Handbook-v2.pdf.

Uiboupin, R., Laanemets, L., Sipelgas, L., Raag, I. Lips, I & Buhhalko, N. (2012). Monitoring the effect ofupwelling on the chlorophyll a distribution in the gulf of Finland (Baltic Sea) using remote sensing and in situdata, *Oceanologia*, 54, (3), 395–419, doi: 10.5697/oc.54-3.395.

U.S. Geological Survey, (2016). Landsat 8 Data Users Handbook, *Nasa*, 8, 97 https://landsat.usgs.gov/documents/Landsat8DataUsersHandbook.pdf.

Vanhellemont, Q. (2021). Automated water surface temperature Landsat 8/TIRS, *Remote Sens.Environ.*, 237, 8 11- 18, doi: 10.1016/j.rse.2019.111518.